

PROCEEDINGS OF SPIE

SPIDigitalLibrary.org/conference-proceedings-of-spie

Characterisation of thermal crosstalk-induced wavelength shift in monolithic InP dual DFB lasers PIC

Lo, Mu-Chieh, Zhou, Zichuan, Pan, Shujie, Carpintero, Guillermo, Liu, Zhixin

Mu-Chieh Lo, Zichuan Zhou, Shujie Pan, Guillermo Carpintero, Zhixin Liu, "Characterisation of thermal crosstalk-induced wavelength shift in monolithic InP dual DFB lasers PIC," Proc. SPIE 11364, Integrated Photonics Platforms: Fundamental Research, Manufacturing and Applications, 113641U (4 May 2020); doi: 10.1117/12.2570618

SPIE.

Event: SPIE Photonics Europe, 2020, Online Only

Characterisation of thermal crosstalk-induced wavelength shift in a monolithic InP dual DFB lasers PIC

Mu-Chieh Lo^a, Zichuan Zhou^a, Shujie Pan^a, Guillermo Carpintero^b, and Zhixin Liu^a

^aUniversity College London, London, UK

^bUniversidad Carlos III de Madrid, Leganés, Spain

ABSTRACT

We present dual DFB lasers each integrated with one heater developed in a generic foundry platform. The thermal effects are experimentally investigated and exhibited a continuous wavelength difference tuning of 0-12.33 nm.

Keywords: Tunable lasers, Thermal effects, Photonic integrated circuits

1. INTRODUCTION

Dual continuous wave (CW) lasers in InP-based C-band photonic integrated circuits (PIC) have become increasingly promising, as they are capable to support the generation of highly advanced modulation format signals,¹ millimeter wave (mmW) and terahertz (THz) carriers.^{2,3} To meet the regulated mmW/THz frequency range and the channel grid given the tight constraints on the wavelength in optical networks, precise spectral tunability of compact devices is essential that is accomplished through injection current tuning and temperature tuning. It is worth mentioning that operation of laser or SOA leads to an additional heating in the gain section, as the thermo-optic coefficient for InP is about $2.5 \times 10^{-4} \text{ }^\circ\text{C}^{-1}$ and thus thermal effects are inherently present.⁴

The thermal effects also give rise to unwanted thermal crosstalk, whereby a component is inevitably influenced by the temperature gradient of a neighbouring heating active component.⁵ Besides considering the thermal management approaches beyond the current standard macroscopic thermo-electric cooling (TEC) and conductive heat transfer, to keep a sufficient distance between components in PIC may significantly reduce the thermal crosstalk.^{6,7} However, it limits the PIC building block density and increases the development cost which conflicts with the concept of photonic integration and generic foundry approach.⁸

In this paper, we demonstrate a monolithically integrated dual DFB laser chip developed in an InP-based generic foundry platform.⁹ The DFB lasers are placed 400 μm from each other in parallel and each one comes with an integrated heater electrode. The thermo-optic tuning capacity and the thermal crosstalk effects of DFB lasers on the DFB laser injection currents and heater currents are experimentally investigated. The dual peak wavelengths and their separation due to the thermal effects are analyzed to provide the thermal characteristics of the foundry technology as toolbox to all generic approach users in their design phase.

Further author information: (Send correspondence to Mu-Chieh Lo)

Mu-Chieh Lo: m.lo@ucl.ac.uk

Guillermo Carpintero: guiller@ing.uc3m.es

Zhixin Liu: zhixin.liu@ucl.ac.uk

Integrated Photonics Platforms: Fundamental Research, Manufacturing and Applications, edited by
Roel G. Baets, Peter O'Brien, Laurent Vivien, Proc. of SPIE Vol. 11364, 113641U
© 2020 SPIE · CCC code: 0277-786X/20/\$21 · doi: 10.1117/12.2570618

2. DEVICE DESCRIPTION

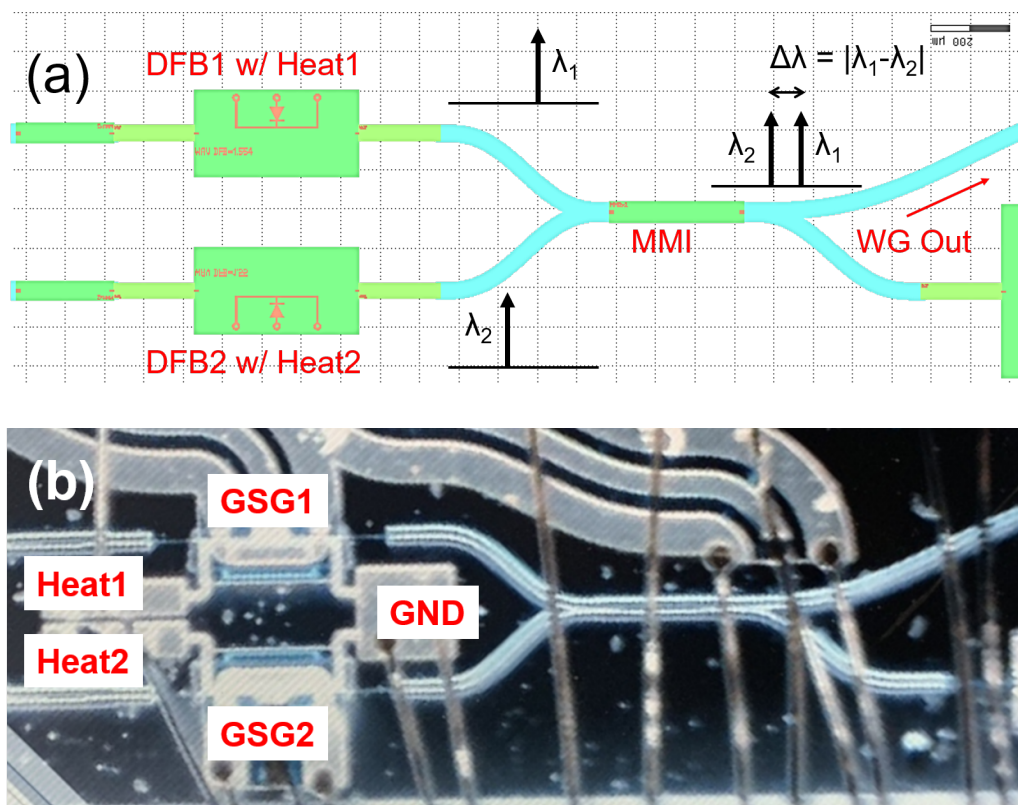


Figure 1. (a) PIC Mask layout. Blue: passive waveguides. Green: DFB laser, shallow-to-deep transition, and coupler building blocks. (b) PIC micro photo. Injection currents and heater currents are fed via GSG1,2 and Heat1,2 electrodes to DFB1 and DFB2, respectively.

The developed PIC mask layout and micro photo are shown in Fig. 1. Fig. 1(a) presents the two freely tunable DFB lasers with heaters are optically coupled through a MMI (multi-mode interference) coupler. Each DFB laser supports both injection current and thermal tuning mechanisms, via the injection current and heater current bonding pads (GSG and Heat, respectively) which are depicted in Fig. 1(b). After the MMI, the combined two wavelengths (λ_1 and λ_2) are delivered to the upper waveguide out (WG Out) on cleaved facet, to which an external fiber is edge-coupled followed by measuring instruments for characterization. Under TEC control at 25 °C the dependency of peak wavelengths λ_1 , λ_2 and wavelength difference $\Delta\lambda = |\lambda_1 - \lambda_2|$ on heater currents (*Heat1* and *Heat2*) and injection currents (*DFB1* and *DFB2*) are collected and analyzed.

3. CHARACTERIZATION RESULTS

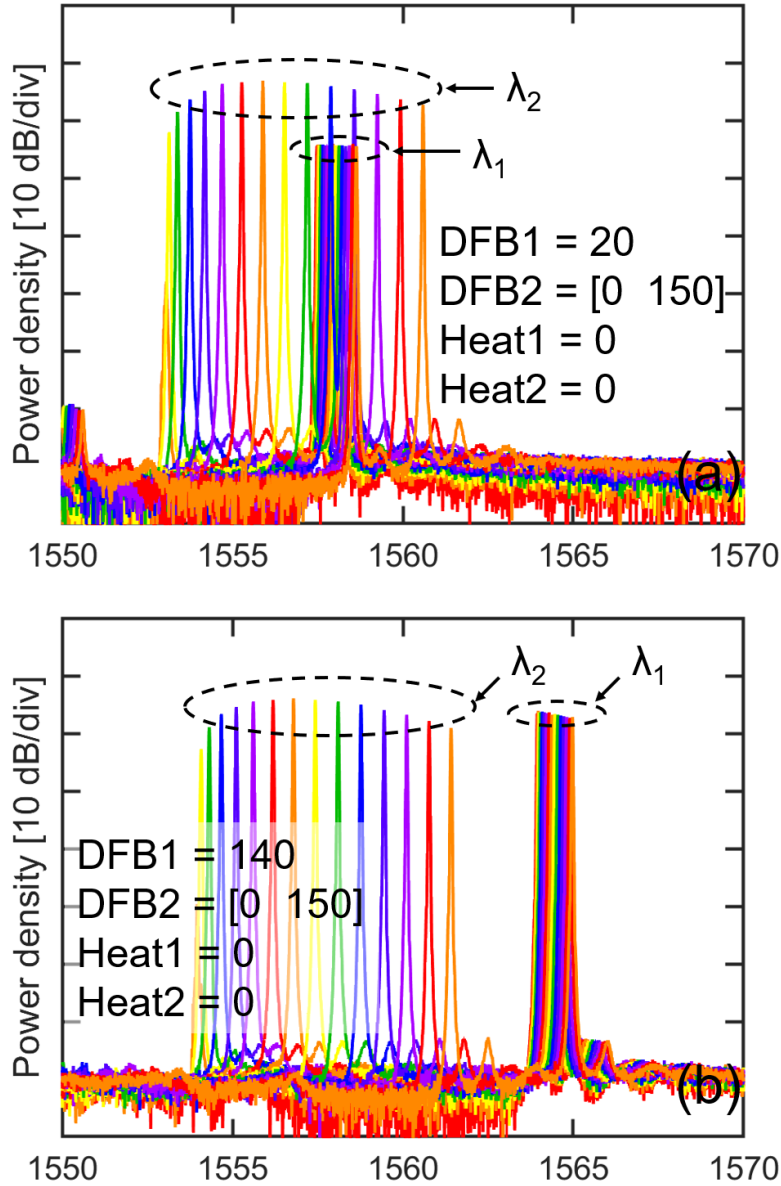


Figure 2. (a) Optical spectra for *DFB1* fixed at 20 mA and *DFB2* varied from 0 to 150 mA. (b) Optical spectra for *DFB1* fixed at 20 mA and *DFB2* varied from 0 to 150 mA.

Fig. 2(a) and Fig. 2(b) present the optical spectrum evolution for *DFB2* driven from 0 to 150 mA with *DFB1* fixed at 20 and 140 mA. Within this range of operation, the peak wavelength of *DFB1* (λ_1) is slightly increased ≈ 1 nm since it is influenced by the heat generated by *DFB2* and the peak wavelength of *DFB2* (λ_2) shifts by ≈ 6 nm. The group of λ_2 in Fig. 2(b) also red-shifts by ≈ 1 nm with respect to that in Fig. 2(a).

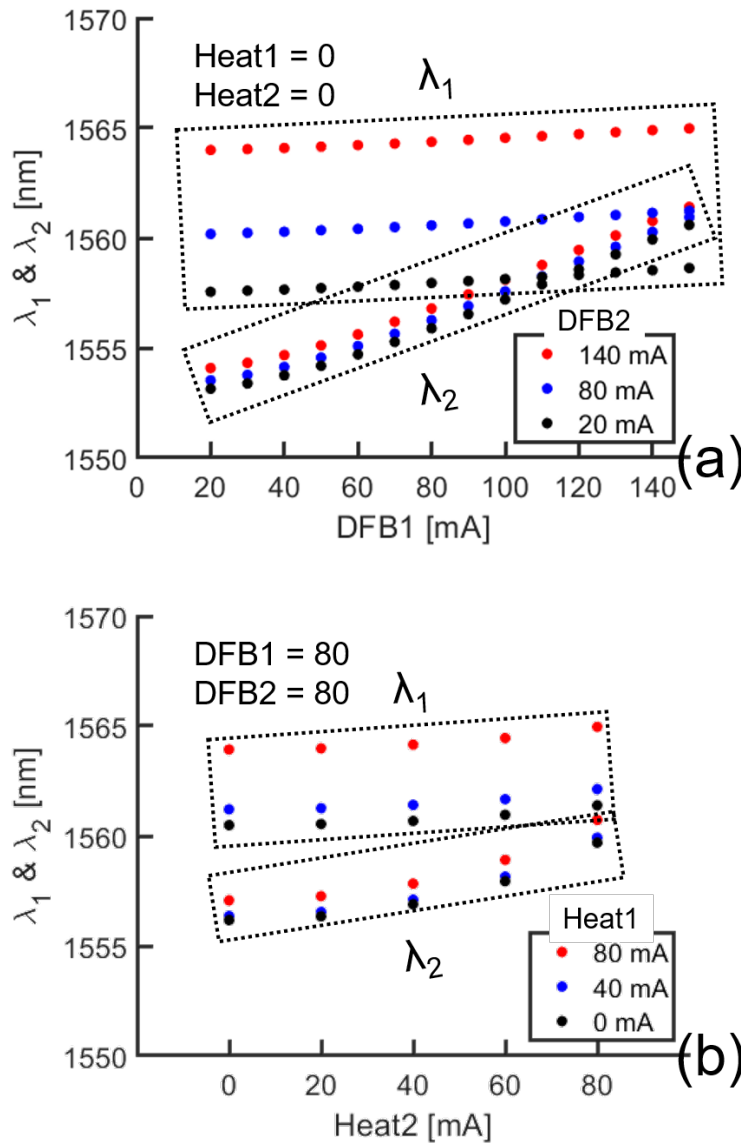


Figure 3. (a) Two peak wavelengths versus $DFB1$ for $DFB2 = 140, 80,$ and 20 mA, and both heaters $Heat1$ and $Heat2$ off. (b) Two peak wavelengths against $Heat2$ for $DFB1 = DFB2 = 80$ mA and $Heat1$ switched off.

By extracting the peak wavelengths from the optical spectra, the dependence of the two peak wavelengths on $DFB1$ injection current is depicted in Fig. 3(a). For $DFB1 = 20, 80,$ and 140 mA, the three sets of dual peak wavelength data exhibit the monotonic upward trend of both λ_1 and λ_2 through the increasing $DFB2$. λ_2 rises more rapidly than λ_1 while $DFB2$ is consistently heating and the different rising rates may lead to wavelength crossing; For instance, when $DFB1 = 20$ mA and $DFB2 \approx 110$ mA the two lasers are in close spectral proximity, indicating the PIC can produce two equal wavelengths if it is properly biased. Similarly, Fig. 3(b) points out λ_1 and λ_2 are both thermally tuned by one single heater of the two, either $Heat1$ or $Heat2$. With a heater current of 80 mA, the corresponding DFB laser red-shifts by ≈ 4 nm and the other DFB laser red-shifts by ≈ 1 nm due to the thermal crosstalk.

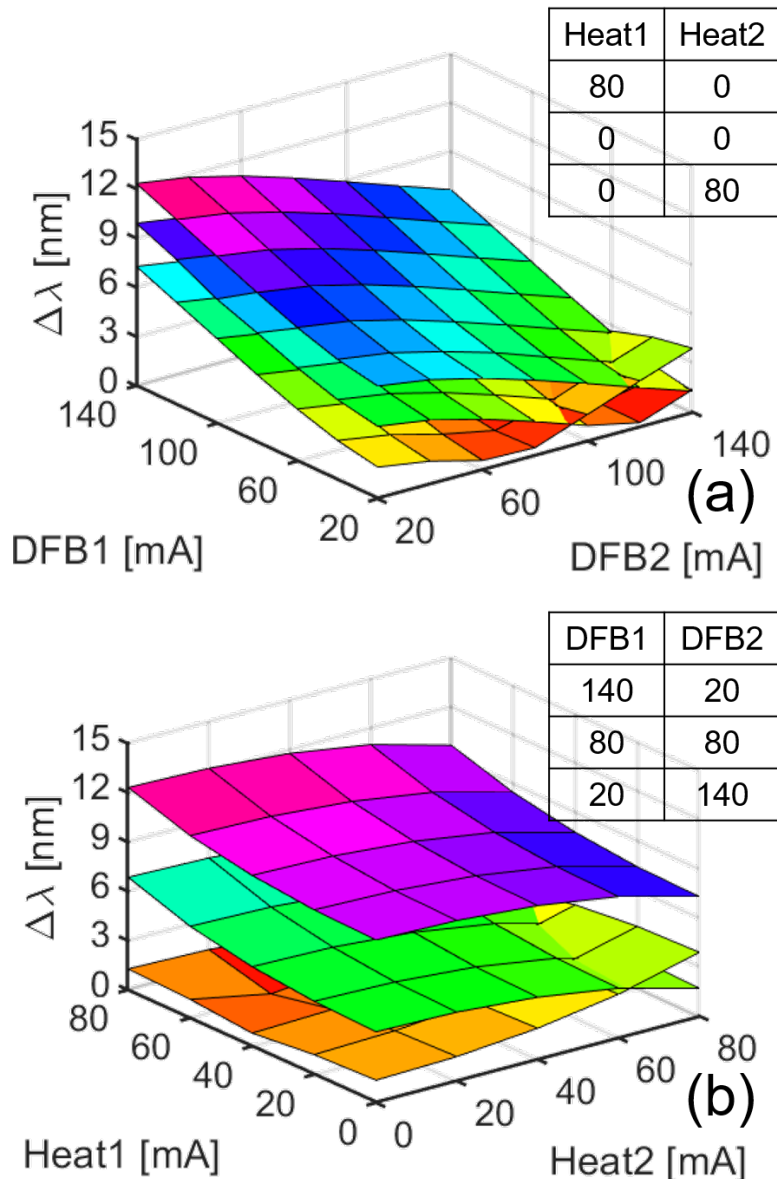


Figure 4. (a) 3D surface plots of wavelength difference against $DFB1$ and $DFB2$. (b) 3D surface plots of wavelength difference against $Heat1$ and $Heat2$.

The wavelength difference ($\Delta\lambda$) is thus associated with the mutual influence, i.e., thermal crosstalk of the four variable factors: $DFB1$, $DFB2$, $Heat1$, and $Heat2$, which is visualized in Fig. 4(a) and Fig. 4(b). By sweeping the four variables, a four-dimension matrix is constructed and can be sliced to demonstrate the spectral information on a certain curved plane of interest. Each plane is composed of a range of linear or nonlinear wavelength dependence data as shown in Fig. 3(a) and Fig. 3(b). Furthermore, the widest $\Delta\lambda$ of 12.33 nm is reached when $DFB1$ and $Heat1$ are operated at the fairly large values (140 and 80 mA) while the $DFB2$ is biased at 20 mA and the heater2 is switched off ($Heat2 = 0$). On the other hand, the turning points of the planes reflect the $\Delta\lambda$ of 0 nm, where the above-mentioned wavelength crossing occurs.

4. CONCLUSIONS

In conclusion, the thermal effects and mutual influences of the PIC have been characterized. For each DFB laser, the tuning ranges of 6 nm and 4 nm for injection current tuning and thermal tuning and the ≈ 1 nm thermal crosstalk from the other laser as well as heater have been obtained. The PIC comprising dual DFB lasers with dual integrated microheaters features a wide tuning range of 0-12.33 nm. Based on the 4D mapping, a pre-compensation scheme is now being evaluated to cancel the thermal crosstalk of the PIC.¹⁰

ACKNOWLEDGMENTS

European Union's Horizon 2020 Marie Skłodowska-Curie grant agreement No.642355 and No.713694; Ministerio de Economía y Competitividad (MINECO) grant iTWIT (TEC2016-76997-C3-3-R) Engineering and Physical Sciences Research Council (EP/R035342/1, EP/R041792/1); Royal Society (PIF/R1/180001).

REFERENCES

- [1] Liu, Z., Kakande, J., Kelly, B., O'Carroll, J., Phelan, R., Richardson, D. J., and Slavík, R., "Modulator-free quadrature amplitude modulation signal synthesis," *Nature communications* **5**, 5911 (2014).
- [2] Carpintero, G., Hisatake, S., de Felipe, D., Guzman, R., Nagatsuma, T., and Keil, N., "Wireless data transmission at terahertz carrier waves generated from a hybrid in-polymer dual tunable dbr laser photonic integrated circuit," *Scientific reports* **8**(1), 3018 (2018).
- [3] Van Dijk, F., Kervella, G., Lamponi, M., Chtioui, M., Lelarge, F., Vinet, E., Robert, Y., Fice, M. J., Renaud, C. C., Jimenez, A., et al., "Integrated inp heterodyne millimeter wave transmitter," *IEEE Photonics Technology Letters* **26**(10), 965–968 (2014).
- [4] Della Corte, F. G., Cocorullo, G., Iodice, M., and Rendina, I., "Temperature dependence of the thermo-optic coefficient of inp, gaas, and sic from room temperature to 600 k at the wavelength of 1.5 μm ," *Applied Physics Letters* **77**(11), 1614–1616 (2000).
- [5] Gilardi, G., Yao, W., Smit, M. K., and Wale, M. J., "Observation of dynamic extinction ratio and bit error rate degradation due to thermal effects in integrated modulators," *Journal of Lightwave Technology* **33**(11), 2199–2205 (2015).
- [6] Sato, K. and Murakami, M., "Experimental investigation of thermal crosstalk in a distributed feedback laser array," *IEEE Photonics technology letters* **3**(6), 501–503 (1991).
- [7] Mathews, I., Abdullaev, A., Lei, S., Enright, R., Wallace, M., and Donegan, J., "Reducing thermal crosstalk in ten-channel tunable slotted-laser arrays," *Optics express* **23**(18), 23380–23393 (2015).
- [8] Smit, M., Leijtsens, X., Ambrosius, H., Bente, E., Van der Tol, J., Smalbrugge, B., De Vries, T., Geluk, E.-J., Bolk, J., Van Veldhoven, R., et al., "An introduction to inp-based generic integration technology," *Semiconductor Science and Technology* **29**(8), 083001 (2014).
- [9] Soares, F. M., Baier, M., Gaertner, T., Grote, N., Moehrl, M., Beckerwerth, T., Runge, P., and Schell, M., "Inp-based foundry pics for optical interconnects," *Applied Sciences* **9**(8), 1588 (2019).
- [10] Milanizadeh, M., Aguiar, D., Melloni, A., and Morichetti, F., "Canceling thermal cross-talk effects in photonic integrated circuits," *Journal of Lightwave Technology* **37**(4), 1325–1332 (2019).